Stable Finite Element Formulation for the Perturbed Convective Wave Equation

Manfred Kaltenbacher[1], **Klaus Roppert**[1], **Stefan Schoder**[1], and **Johannes Heinz**[2]

[1]Institute of Fundamentals and Theory in Electrical Engineering, TU Graz, Austria
({manfred.kaltenbacher,klaus.roppert,stefan.schoder}@tugraz.at)

[2]Institute of Mechanics and Mechatronics, TU Wien, Austria
(johannes.heinz@tuwien.ac.at)

Abstract
In computational aeroacoustics for low Mach numbers, the acoustic perturbation equations (APE) allow for a precise separation between the physical flow quantities and the acoustic quantities. By introducing the acoustic scalar potential, this set of partial differential equations can be rewritten without any approximations by the Perturbed Convective Wave Equation (PCWE). This second order partial differential equation in space and time fits well to be solved by the Finite Element (FE) method. However, one has to take care that the convective operator, which is non-symmetric, is formulated in such a way that the discrete system preserves non-symmetry. Otherwise, spurious modes occur, which will strongly disturb the numerical solution and the computation may even become unstable.

Keywords: Convective wave equation, preserving non-symmetry, finite elements

1 Introduction

The convective wave equation (CWE) describes acoustic wave propagation in flowing media. A systematic derivation of CWE has been provided in [1] starting at the full set of compressible flow equations and applying a perturbation ansatz. The final partial differential equation is similar to the standard wave equation, but instead of the second order partial time derivative it has a second order substantial time derivative. Thereby, it has been assumed that the medium is slowly varying both with position over distances and over times compared to the wavelength and representative acoustic period, respectively. For application of this convective wave equation we refer, e.g., to the simulation of ultrasonic flow meters [2], where the background flow is assumed to be independent of time.

Recently, in computational aeroacoustics, the reformulation of the acoustic perturbation equations (APE) leads to the same convective wave operator and the substantial derivative of the incompressible flow pressure as a source term. This partial differential equation has again the scalar acoustic potential as the search for quantity and has been named perturbed acoustic wave equation (PCWE) [3, 4, 5, 6, 7]

In our contribution, we show the derivation of a stable FE formulation by applying an appropriate transformation of the standard FE formulation. Furthermore, we demonstrate by an eigenvalue analysis the strong reduction of the real part of the eigenvalues, and benchmark the numerical computation by an example with analytical solution.

2 Finite Element Formulation

We consider the following homogeneous convective wave equation

$$\frac{1}{c_0^2}\,\frac{\mathrm{D}^2\psi}{\mathrm{D}t^2} - \nabla\cdot\nabla\psi = 0\,; \qquad \frac{\mathrm{D}}{\mathrm{D}t} = \frac{\partial}{\partial t} + \overline{\boldsymbol{u}}\cdot\nabla\,. \tag{1}$$

It has been derived in [1] for the case of sound in fluids with unsteady inhomogeneous flow as well as in [3] for modeling aeroacoustics phenomena. In (1), ψ denotes the scalar acoustic potential, c_0 the speed of sound in the medium and $\overline{\boldsymbol{u}}$ the mean flow velocity (constant in time). In a next step, we derive the weak formulation. In doing so, we introduce an appropriate test function φ, multiply (1) by it and integrate over the whole computational domain Ω

$$\frac{1}{c_0^2}\int\limits_\Omega \varphi\,\frac{\mathrm{D}^2\psi}{\mathrm{D}t^2}\,\mathrm{d}\boldsymbol{x} - \int\limits_\Omega \varphi\,\nabla\cdot\nabla\psi\,\mathrm{d}\boldsymbol{x} = 0\,. \tag{2}$$

Expanding the substantial derivative in (2) results in five terms

$$\underbrace{\frac{1}{c_0^2}\int\limits_\Omega \varphi\,\frac{\partial^2\psi}{\partial t^2}\,\mathrm{d}\boldsymbol{x}}_{I} + \underbrace{\frac{1}{c_0^2}\int\limits_\Omega \varphi\,\big(\overline{\boldsymbol{u}}\cdot\nabla\big)\,\frac{\partial\psi}{\partial t}\,\mathrm{d}\boldsymbol{x}}_{IIa} + \underbrace{\frac{1}{c_0^2}\int\limits_\Omega \varphi\frac{\partial}{\partial t}\big(\overline{\boldsymbol{u}}\cdot\nabla\,\psi\big)\,\mathrm{d}\boldsymbol{x}}_{IIb}$$
$$+\underbrace{\frac{1}{c_0^2}\int\limits_\Omega \varphi\,\big(\overline{\boldsymbol{u}}\cdot\nabla\big)\big(\overline{\boldsymbol{u}}\cdot\nabla\big)\,\psi\,\mathrm{d}\boldsymbol{x}}_{III} + \underbrace{\int\limits_\Omega \varphi\,\nabla\cdot\nabla\psi\,\mathrm{d}\boldsymbol{x}}_{IV} = 0\,. \tag{3}$$

The term I is a standard bilinear form and needs no special treatment. However, the terms IIa and IIb are subjected to the mean flow field, which is not necessarily homogeneous. By exploring the property that the mean flow $\overline{\boldsymbol{u}}$ is time-independent, the two terms IIa and IIb in (3) may be combined to

$$\int\limits_\Omega \varphi\,\big(\overline{\boldsymbol{u}}\cdot\nabla\big)\,\frac{\partial\psi}{\partial t}\,\mathrm{d}\boldsymbol{x} + \frac{1}{c_0^2}\int\limits_\Omega \varphi\frac{\partial}{\partial t}\big(\overline{\boldsymbol{u}}\cdot\nabla\,\psi\big)\,\mathrm{d}\boldsymbol{x} = \frac{2}{c_0^2}\int\limits_\Omega \varphi\,\big(\overline{\boldsymbol{u}}\cdot\nabla\big)\,\frac{\partial\psi}{\partial t}\,\mathrm{d}\boldsymbol{x}\,. \tag{4}$$

As pointed out in [8], the skew symmetry of the operator has to be preserved in the discrete form, in order to achieve energy conservation and stability. The eigenvalue analysis in Sec. 3 will demonstrate that spurious modes arise and some of them even with positive real part, so that unstable computations are observed. Therefore, we split the term (4) in two equal terms and perform an integration by parts to one of them. In doing so, the integration by parts results in

$$\begin{aligned}\int\limits_\Omega \varphi\,(\overline{\boldsymbol{u}}\cdot\nabla)\,\frac{\partial\psi}{\partial t}\;\mathrm{d}\boldsymbol{x} &= -\int\limits_\Omega \nabla\cdot(\varphi\,\overline{\boldsymbol{u}})\,\frac{\partial\psi}{\partial t}\;\mathrm{d}\boldsymbol{x} + \int\limits_\Gamma \varphi\,(\overline{\boldsymbol{u}}\cdot\boldsymbol{n})\,\frac{\partial\psi}{\partial t}\;\mathrm{d}\boldsymbol{s} \\ &= -\int\limits_\Omega \frac{\partial\psi}{\partial t}\,(\overline{\boldsymbol{u}}\cdot\nabla)\,\varphi\;\mathrm{d}\boldsymbol{x} + \int\limits_\Gamma \varphi\,(\overline{\boldsymbol{u}}\cdot\boldsymbol{n})\,\frac{\partial\psi}{\partial t}\;\mathrm{d}\boldsymbol{s}\;. \qquad (5)\end{aligned}$$

Here, the derivation just holds for the case that $\overline{\boldsymbol{u}}$ is incompressible or in an FE setting, where $\overline{\boldsymbol{u}}$ is piecewise constant for each finite element. Exploring this result, we may rewrite (4) using (5) by

$$\begin{aligned}\frac{2}{c_0^2}\int\limits_\Omega \varphi\,(\overline{\boldsymbol{u}}\cdot\nabla)\,\frac{\partial\psi}{\partial t}\;\mathrm{d}\boldsymbol{x} &= \frac{1}{c_0^2}\int\limits_\Omega \varphi\,(\overline{\boldsymbol{u}}\cdot\nabla)\,\frac{\partial\psi}{\partial t}\;\mathrm{d}\boldsymbol{x} \\ &\quad -\frac{1}{c_0^2}\int\limits_\Omega \frac{\partial\psi}{\partial t}\,(\overline{\boldsymbol{u}}\cdot\nabla)\,\varphi\;\mathrm{d}\boldsymbol{x} + \frac{1}{c_0^2}\int\limits_\Gamma \varphi\,(\overline{\boldsymbol{u}}\cdot\boldsymbol{n})\,\frac{\partial\psi}{\partial t}\;\mathrm{d}\boldsymbol{s}\,, \quad (6)\end{aligned}$$

which will guarantee skew symmetry also in the space discrete form.

The term III is also integrated by parts, and for the same assumption towards the mean flow velocity $\overline{\boldsymbol{u}}$ as before, we arrive at

$$\begin{aligned}\frac{1}{c_0^2}\int\limits_\Omega \varphi\,(\overline{\boldsymbol{u}}\cdot\nabla)(\overline{\boldsymbol{u}}\cdot\nabla)\,\psi\;\mathrm{d}\boldsymbol{x} &= \frac{1}{c_0^2}\int\limits_\Omega \nabla(\overline{\boldsymbol{u}}\,\varphi)\,(\overline{\boldsymbol{u}}\cdot\nabla)\,\psi\;\mathrm{d}\boldsymbol{x} \\ &= -\frac{1}{c_0^2}\int\limits_\Omega (\overline{\boldsymbol{u}}\cdot\nabla)\,\varphi\,(\overline{\boldsymbol{u}}\cdot\nabla)\,\psi\;\mathrm{d}\boldsymbol{x} \\ &\quad +\frac{1}{c_0^2}\int\limits_\Gamma \varphi\,(\overline{\boldsymbol{u}}\cdot\boldsymbol{n})\,(\overline{\boldsymbol{u}}\cdot\nabla)\psi\;\mathrm{d}\boldsymbol{s}\,. \qquad (7)\end{aligned}$$

The term IV in (3) is treated as usual and results in

$$\int\limits_\Omega \varphi\,\nabla\cdot\nabla\psi\;\mathrm{d}\boldsymbol{x} = -\int\limits_\Omega \nabla\varphi\cdot\nabla\psi\;\mathrm{d}\boldsymbol{x} + \int\limits_\Gamma \varphi\,\boldsymbol{n}\cdot\nabla\psi\;\mathrm{d}\boldsymbol{s}\,. \qquad (8)$$

Collecting all the performed steps, the weak formulation of (1) reads as follows (assuming $\overline{\boldsymbol{u}}\cdot\boldsymbol{n} = 0$): Find $\psi \in H^1$ such that

$$\begin{aligned}&\frac{1}{c_0^2}\int\limits_\Omega \varphi\,\frac{\partial^2\psi}{\partial t^2}\;\mathrm{d}\boldsymbol{x} + \frac{1}{c_0^2}\int\limits_\Omega \varphi\,(\overline{\boldsymbol{u}}\cdot\nabla)\,\frac{\partial\psi}{\partial t}\;\mathrm{d}\boldsymbol{x} - \frac{1}{c_0^2}\int\limits_\Omega \frac{\partial\psi}{\partial t}\,(\overline{\boldsymbol{u}}\cdot\nabla)\,\varphi\;\mathrm{d}\boldsymbol{x} \\ &-\frac{1}{c_0^2}\int\limits_\Omega (\overline{\boldsymbol{u}}\cdot\nabla)\,\varphi\,(\overline{\boldsymbol{u}}\cdot\nabla)\,\psi\;\mathrm{d}\boldsymbol{x} - \int\limits_\Omega \nabla\varphi\cdot\nabla\psi\;\mathrm{d}\boldsymbol{x} + \int\limits_\Gamma \varphi\,\boldsymbol{n}\cdot\nabla\psi\;\mathrm{d}\boldsymbol{s} = 0 \qquad (9)\end{aligned}$$

is fulfilled for all $\varphi \in H_0^1$.
Applying a standard FE ansatz with appropriate FE basis functions $N_i(\boldsymbol{x})$

$$\varphi \approx \varphi^h = \sum_i N_i(\boldsymbol{x})\,\varphi_i(t)\,; \quad \psi \approx \psi^h = \sum_k N_k(\boldsymbol{x})\,\psi_k(t) \qquad (10)$$

results in the following semi-discrete Galerkin formulation

$$\boldsymbol{M}\ddot{\underline{\psi}}^h + \boldsymbol{C}\dot{\underline{\psi}}^h + \boldsymbol{K}\underline{\psi}^h = \underline{f}^h \,. \tag{11}$$

In (11) $\underline{\psi}^h$ denotes an algebraic vector collecting all the unknowns of the scalar acoustic potential and a dot over a variable denotes the derivative with respect to time, i.e. $\partial^2\underline{\psi}^h/\partial t^2 = \ddot{\underline{\psi}}^h$, and $\underline{f}^h$ the right hand side according to a given source term or boundary conditions. Furthermore, in (11) $\boldsymbol{M}, \boldsymbol{C}, \boldsymbol{K} \in \mathbb{R}^{n_{\mathrm{eq}}} \times \mathbb{R}^{n_{\mathrm{eq}}}$ are the mass, damping and stiffness matrices with n_{eq} the number of unknowns. The time discretization is performed by a classical Newmark method or in order to achieve second order temporal accuracy by the Hilber–Hughes–Taylor (HHT) method [10].

3 Eigenvalue Analysis

For the investigation of spurious modes, we perform computations for plane waves in a channel of length L with uniform background flow (see Fig. 1). As boundary conditions, we set $\psi(t, x = 0) = 0$ and $\psi(t, x = L) = 0$. For this case, the convective wave equation (1) may be rewritten as [11]

$$\frac{\partial^2\psi}{\partial t^2} + 2Mc_0\frac{\partial^2\psi}{\partial x\partial t} + (M^2-1)c_0^2\frac{\partial^2\psi}{\partial x^2} = 0\,. \tag{12}$$

In (12) M denotes the Mach number computed by

$$M = \frac{||\overline{\boldsymbol{u}}||}{c_0}\,.$$

For the solution, we choose the ansatz

$$\psi(x,t) = \hat{\psi}\, e^{j(k\;x-\omega t)}$$

with k the the wave number, ω the angular frequency and j the complex unit. Substituting this ansatz into (12), results in the solution for k by fixed ω

$$k_{1,2} = -\frac{\omega\big(M\,c_0 \mp c_0\big)}{\big(M^2\,c_0^2 - c_0^2\big)} = -\frac{\omega}{(M\pm 1)\,c_0}\,. \tag{13}$$

By considering the boundary conditions, one obtains the following analytical eigenvalues

$$\omega_n = \frac{c_0\pi n}{L}(1-M^2)\,. \tag{14}$$

To compute the discrete eigenvalues of (11), we set

$$\underline{\psi}^h = \Psi\, e^{st}\,;\;\; s = j\omega$$

and substituting it into (11) results in

$$\big(s^2\boldsymbol{M} + s\boldsymbol{C} + \boldsymbol{K}\big)\;\Psi = \boldsymbol{0}\,. \tag{15}$$

This equation is satisfied by the i-th latent root s_i, and i-th latent vector $\underline{\Psi}$ of the λ-matrix problem [12], so that

$$s_i^2\boldsymbol{M}\underline{\Psi}_i + s_i\boldsymbol{C}\underline{\Psi}_i + \boldsymbol{K}\underline{\Psi}_i = \boldsymbol{0}\;\;\forall_i \in 1...n_{\mathrm{eq}}\,. \tag{16}$$

For the numerical computation, we have computed the matrices by our open source research software openCFS [13] and then applied Matlab using the function *polyeig*. The first smallest non zero eigenvalues should correspond with the frequencies of the one dimensional channel, i.e. $\lambda \simeq j\omega_n$ (higher values of λ correspond to eigenfunctions oscillating in the height H of the channel). Thereby, the discrete eigenvalues can be interpreted as follows:

- If there are eigenvalues λ, which do not match the analytical ones, we can say that these are spurious modes.

- If the discrete eigenvalues have a positive real part, the solution becomes unstable.

- Spurious modes with a large negative real part are quickly damped and do not disturb the solution.

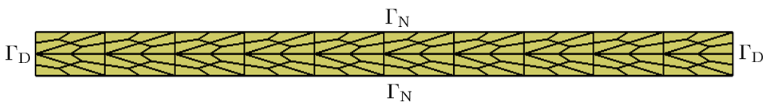

Figure 1 – Pseudo one dimensional channel with strongly distorted elements.

For the numerical evaluation of the discrete eigenvalues a long and thin channel with a length to width ratio of 20 : 1 is chosen. The channel is discretized with distorted quadrilateral elements as displayed in Fig. 1.

Initially the flow velocity is set to zero, which means that the eigenvalues of the standard wave equation are computed (no convective terms). All computed discrete eigenvalues are at the imaginary axis, and have zero real part and coincide with the analytical ones.

In contrast to the stable computations with zero Mach number the situation looks different when a constant mean flow of Mach numbers 0.1, 0.2, 0.3 is present. In a first step, we use the standard formulation, which does not utilize an integration of parts by term IIa, IIb. Therefore, the skew symmetry is not preserved at the discrete level. As demonstrated by Fig. 2 (left plot), a lot of spurious modes are added to the system. Even more dramatically, spurious modes with large positive real part occur which are responsible for unstable computations. In a second step, we perform the computation of the advanced formulation, for which an integration of parts is performed for the terms IIa, IIb. Thereby, the skew symmetry is preserved also on the discrete level. Figure 2 (right plot) displays the computed eigenvalues, and as one can see, the real part of the eigenvalues have been reduced by several magnitudes, and do not increase with higher Mach numbers.

4 Benchmark

As a benchmark example, a setup introduced in [14] is chosen as depicted in Fig. 3. Actually, this benchmark example (see category 4, problem 1 defined by *Reflection*

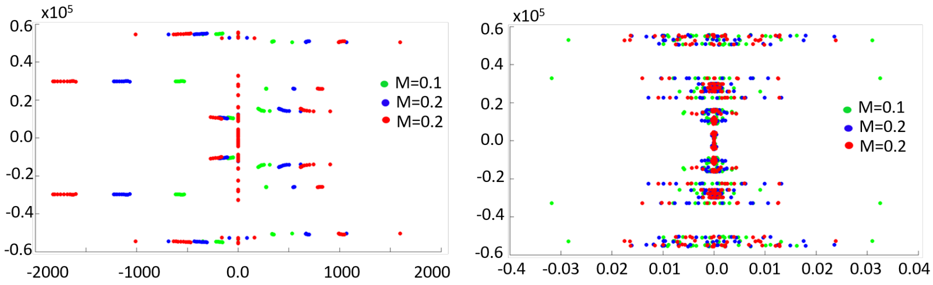

Figure 2 – Discrete eigenvalues for different Mach numbers for standard (left) and enhanced (right) formulation.

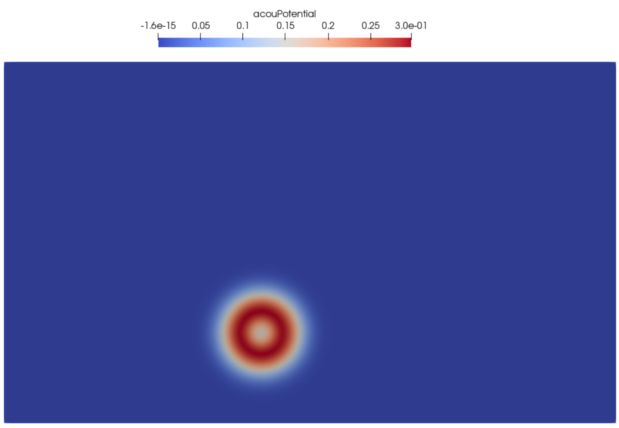

Figure 3 – Computational setup with plotted initial acoustic scalar potential distribution.

of an acoustic pulse off a wall in the presence of a uniform flow in semi-infinite space) has been setup to investigate numerical solution methods for the linearized Euler equations (LEE). Thereby, it can be shown that the LEE for this case can be reformulated for the pressure p by the convective wave equation as formulated in (1) for the scalar acoustic potential ψ. This allows us to use the analytical solution of the pressure p and interpret it as the analytical solution for the acoustic scalar potential ψ. For the computation, a uniform background flow of $\overline{\boldsymbol{u}} = (0.3c_0, 0)^T$ is prescribed resulting in a Mach number of $M = 0.3$. The computational domain is of size 170 m by 100 m. In doing so, the scalar acoustic potential and its first order time derivative at $t = 0$ are given by

$$\psi(\boldsymbol{x}, 0) = e^{\left(\ln(2)\frac{x^2+(y+25)^2}{25}\right)^2} \tag{17}$$

$$\frac{\partial \psi}{\partial t} = -M\frac{\partial \psi}{\partial x}|_{t=0} = \frac{2xM\ln(2)}{25}e^{\left(\ln(2)\frac{x^2+(y+25)^2}{25}\right)^2} . \tag{18}$$

During the pulse propagation, the acoustic pressure is recorded along the monitoring line plotted in Fig. 3. The domain is discretized by finite elements with basis function of first order and an edge length of approximately $h = 0.5\,\mathrm{m}$ and a HHT time stepping scheme is use (the difference to a standard Newmark time stepping scheme is negligible). According to [14], the analytical solution for the acoustic scalar potential computes by

$$\psi(\boldsymbol{x}, t) = \frac{1}{2\alpha} \int_0^\infty e^{-\frac{\xi^2}{4\alpha}} \cos(\xi t) \Big(J_0(\xi\eta) + J_0(\xi\zeta) \Big) \xi \, \mathrm{d}\xi \,. \tag{19}$$

In (19) J_0 denotes the Bessel function of first kind, and the parameters compute by

$$\begin{aligned} \alpha &= \frac{\ln(2)}{25}\,, \\ \eta &= \sqrt{(x - Mt)^2 + (y - 25)^2}\,, \\ \zeta &= \sqrt{(x - Mt)^2 + (y + 25)^2}\,. \end{aligned}$$

The acoustic potential distribution at $t = 60\,\mathrm{s}$ is displayed in Fig. 4. Furthermore, the acoustic scalar potential ψ is evaluated along the line as shown in Fig. 4 and compared to the analytical solution. In doing so, we obtain Fig. 5 demonstrat-

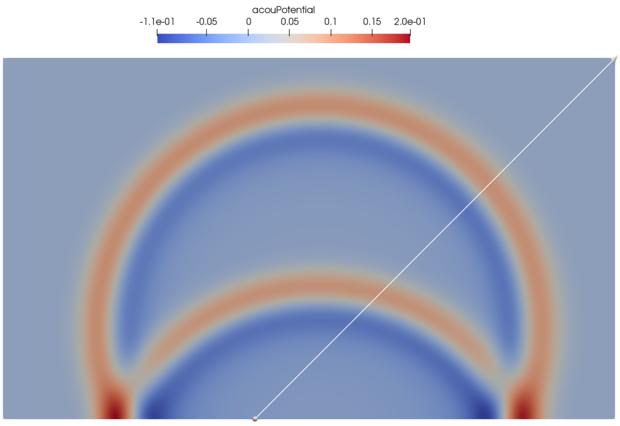

Figure 4 – Computed acoustic potential with marked evaluation line.

ing a perfect match between numerical and analytical results for all investigated Mach numbers. Therefore, the presented approach provides accurate and stable results.

Acknowledgements

This project has received funding from the European Union's Framework Programme for Research and Innovation Horizon 2020 (2014–2020) under the Marie Skłodowska-Curie Grant Agreement No. [812719].

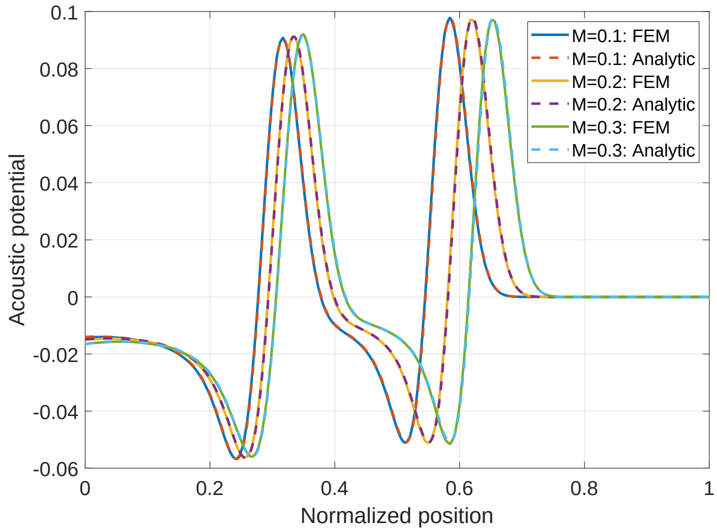

Figure 5 – Computed and analytic results for the three Mach numbers along the line as defined in Fig. 4.

References

[1] A. D. Pierce: Wave equation for sound in fluids with unsteady inhomogeneous flow. J. Acoust. Soc. Am. 87, 2292, 1990

[2] M. Bezdek, H. Landes, A. Rieder, R. Lerch: A Coupled Finite-Element, Boundary-Integral Method for Simulating Ultrasonic Flowmeters. IEEE transactions on ultrasonics, ferroelectrics, and frequency control, vol. 54, no 3, 2007

[3] M. Kaltenbacher, A. Hüppe, A. Reppenhagen, F. Zenger, S. Becker: Computational Aeroacoustics for Rotating Systems with Application to an Axial Fan. AIAA 55(11), 2017

[4] F. Zenger, C. Junger, M. Kaltenbacher, S. Becker: Investigation of the flow- and sound-field of a low-pressure axial fan benchmark case using experimental

and numerical methods. Journal of the Acoustical Society of America, vol 141, 2017

[5] M. Tautz, K. Besserer, S. Becker, M. Kaltenbacher: Source Formulations and Boundary Treatments for Lighthill's Analogy Applied to Incompressible Flows. AIAA Journal, vol. 56, no. 7, 2018

[6] S. Schoder, M. Kaltenbacher: Hybrid Aeroacoustic Computations: State of Art and New Achievements. Journal of Theoretical and Computational Acoustics, vol. 27, no.4 , 2019

[7] S. Schoder, P. Maurerlehner, A. Wurzinger, A. Hauser, S. Falk, S. Kniesburges, M Döllinger, M. Kaltenbacher: Aeroacoustic Sound Source Characterization of the Human Voice Production-Perturbed Convective Wave Equation. Applied Sciences, vol. 11, no. 6, 2021

[8] Y. Morinishi: Skew-symmetric form of convective terms and fully conservative finite difference schemes for variable density low-mach number flows. Journal of Computational Physics 229, 2010

[9] A. Hüppe, G. Cohen, S. Imperiale, M. Kaltenbacher: Construction and Analysis of an Adapted Spectral Finite Element Method to Convective Acoustic Equations. Communications in Computational Physics, 20(1), 2016

[10] Hughes, T. J. R., The Finite Element Method, Dover Publ., Mineola, New York, 2000, pp. 532–535.

[11] A. Hüppe: Spectral Finite Elements for Acoustic Field Computation. Ph.D. thesis, Alps Adriatic University, Austria, 2013

[12] P. Lancaster: Lambda-Matrices and Vibrating System. Pergamon Press, London, 1966

[13] M. Kaltenbacher: Numerical Simulation of Mechatronic Sensors and Actuators: Finite Elements for Multiphysics. Springer-Verlag, Heidelberg, 3rd edition, 2015

[14] C. K. Tam. Benchmark problems and solutions. In ICASE/LaRC Workshop on Benchmark Problems in Computational Aeroacoustics, 1995.